Lasers in Manufacturing Conference 2025

Laser Beam Welding of Additive Manufactured (L-PBF) Aluminium AlSi7Mg0.6 and AlZn5.5MgCu: Welding Process and Properties

Benjamin Keßler[1], Thomas Kairet[2], Olivier Rigo[2], Pierre Billy[3], Petra Svarova[3], Axel Jahn[1], Dirk Dittrich[1]

[1]*Fraunhofer Institut for Material and Beam Technology IWS, Winterbergstraße 28, 01277 Dresden, Germany*
[2] *Sirris, Belgium*
[3] *CRM group, Belgium*

Abstract

The cost aspect is becoming increasingly important in the manufacturing of complex additively manufactured components. One method of reducing costs is hybrid design, i.e. combining semi-finished products with the additively manufactured components. For this reason, the focus is on welding processes to improve overall performance of the final component. Laser welding is particularly suitable for joining components to avoid subsequent processes issues such as distortion due to the low heat input.
As part of the study, the aluminum alloys AlZn5.5MgCu (EN AW-7075) and AlSi7Mg0.6 (EN AC-42200) were used to build components using L-PBF and to weld them using laser high-frequency beam oscillation. That approach enables hot-crack free weld seams and provides high process stability towards avoidance of melt pool blow-outs. The paper shows the developed process approach and resulting properties (microstructure of the weld, tensile strength and fatigue strength) were compared with alternative welding processes (FSW, EBW and GTAW).

Keywords: laser beam welding; aluminium, additive manufacturing, laser powder bed fusion, mechanical properties

1. Introduction

Additive manufacturing has established itself as a significant growth market in recent years, offering innovative solutions for the production of complex components. Among the various processes, Laser Powder Bed Fusion (L-PBF) has emerged as the most widely used manufacturing method for metallic additively manufactured components, including aluminium alloys. Despite the promising possibilities of these technologies, companies face the challenge of high production costs resulting from lengthy processing times and powder material expenses. These financial barriers have so far limited widespread application across many industries.
As a consequence of these economic constraints, a shift in focus from technological innovations to cost reduction has become evident. This paper presents a solution that combines the advantages of additive manufacturing with the benefits of standard semi-finished products. By integrating additively manufactured sections that enable complex geometries and functional integration with standardized, high-strength semi-finished products characterized by solid structures and simple production, significant advancements in cost optimization can be achieved.

2. Materials and Methods

The selection of materials can be found in Table 1. The alloy AlSi7Mg0.6 has been chosen for the automotive industry, while the alloy AlZn5.5MgCu is specifically targeted for the aerospace industry. To enhance the printability of the AlZn5.5MgCu powder, a modification with a Ti-PVD coating has been applied, allowing for grain refinement. Additionally, AlSi7Mg0.6 has been welded to a standard alloy, EN AW-5083, for demonstration purposes [1].

Table 1

No.	*AM Part (L-PBF)*	*Corresponding to*	*Properties*
1	AlSi7Mg0.6	EN AC-42200	High strength-to-weight ratio, good corrosion resistance, surface finish similar to die casting
2	AlZn5,5MgCu	EN AW-7075	Aircraft industry, Innovation: Ti-Coating of the powder, Improved printability and weldability

For the investigation and development of the welding process, plates with a thickness of 3 mm were produced using the laser powder bed fusion (L-PBF) method and subsequently machined at the joining edge.
All plates have been printed on an SLM280 (Nikon SLM solutions). Process parameters for the printing of AlSi7Mg06 can be found in reference [2] while process parameters for AlZn5.5MgCu can be found in reference [3].
The welding trials were conducted utilizing specialized equipment designed to meet industrial standards. A key component of the setup was a 5-axis CNC gantry machine, which enabled precise control over the welding process. The primary source of welding energy was a single-mode fiber laser with a maximum output power of 5 kW, facilitating efficient and effective welding operations.
To enhance both the accuracy and speed of the welding process, a galvanometer scanner was incorporated into the setup. This scanner was capable of achieving a maximum oscillation frequency of 4 kHz with an oscillation amplitude of 0.15 mm, allowing for fine adjustments during welding. The focus diameter of the laser was set at 38 µm, which is critical for producing high-quality welds with minimal heat-affected zones.
Argon gas was employed as the protective atmosphere during the welding trials, ensuring that the weld area remained free from contaminants that could compromise weld integrity. Additionally, a pneumatic clamping device was used to secure the workpieces in place, providing stability throughout the welding process.
It is noteworthy that the Rayleigh length for the laser was measured to be less than 1 mm, indicating a high sensitivity of the welding process to variations in setup and environmental conditions. This sensitivity underscores the importance of precise control and monitoring during the welding trials to achieve optimal results. The experimental setup is illustrated in Fig. 1.

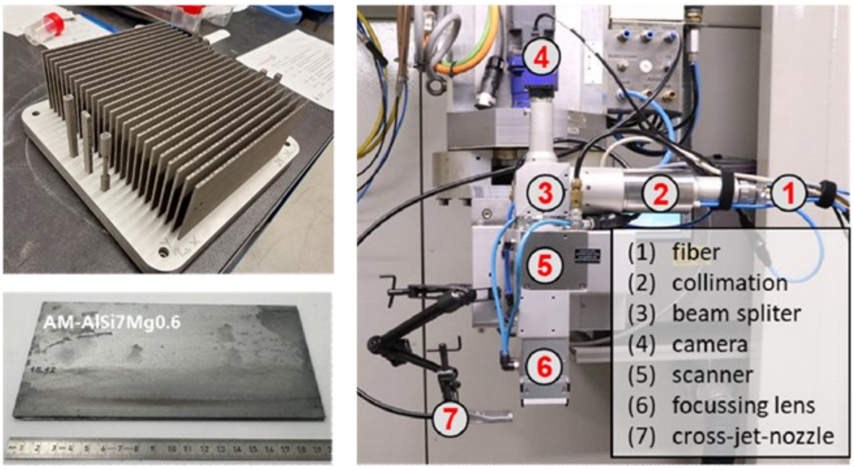

Fig. 1: left top: example of printed sheet material; left down: separated printed plate from AlSi7Mg0,6 and right: experimental set-for laser beam welding

3. Results

3.1. Laser process investigations

During the project, the hypothesis that the process approach is applicable to the welding of additively manufactured (AM) components was successfully validated using a synchrotron source at the TOMCAT beamline of the Swiss Light Source (SLS) at the Paul Scherer Institute (PSI) in Villigen, Switzerland [4].

For the AlSi7Mg0.6 alloy, a key finding was that the phenomenon of keyhole widening is also relevant for materials produced via the laser powder bed fusion (L-PBF) process. Figure 2 illustrates a comparison of three weld trials conducted on AlSi7Mg0.6, all utilizing the same laser beam power and welding speed, while varying the oscillation frequency (0 Hz, 1000 Hz, and 4000 Hz). It was observed that at an oscillation frequency of 4000 Hz, the keyhole is widened, facilitating improved degassing of the molten material. Consequently, the process approach was further investigated throughout the study.

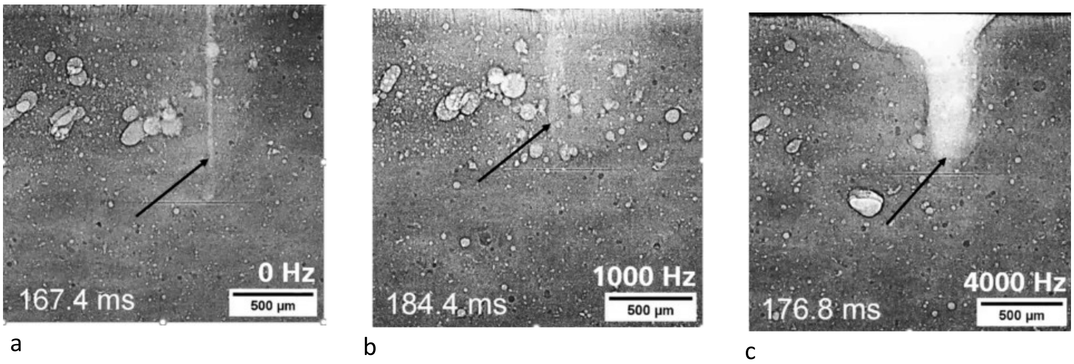

Fig. 2 Welding trials in AlSi7Mg0.6 (a) with static laser beam (local keyhole); (b) 1000 Hz oscillation frequency (modulated key hole); (c) 4000 Hz oscillation frequency (expanded keyhole)

Fig. 3 shows exemplary cross-sections of weld seams between AlSi7Mg0,6 and EN AW-5083. It can be seen that the pore distribution is random and should not only be evaluated in the cross-section. However, the existing pores are fine and spread across the weld seam uniformly, so that they probably do not originate from the process but from the base material. Both weld seams show no cracks and good mixing of the materials.

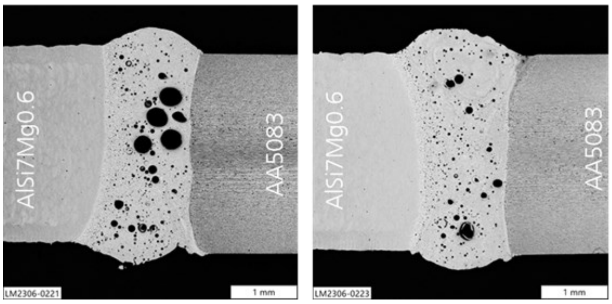

Fig. 3 Butt-joints of AlSi7Mg0.6 and EN AW-5083

In the progress of the process development, there were also strong differences in the weld seam quality of the AM-material. It was assumed that the hydrogen content in the additively manufactured base material varied significantly. For this reason, samples were taken from AM samples and subjected to hot gas extraction. A high hydrogen content of 22 ppm was detected in the base material of the weld seam in Fig. 4. This is reflected in the fine distribution of pores in the weld seam.

The cause of the hydrogen contamination could not be clarified and is the subject of further investigations. For the industrial user, however, it was possible to show that this is an influencing parameter for the weld seam quality that should not be neglected.

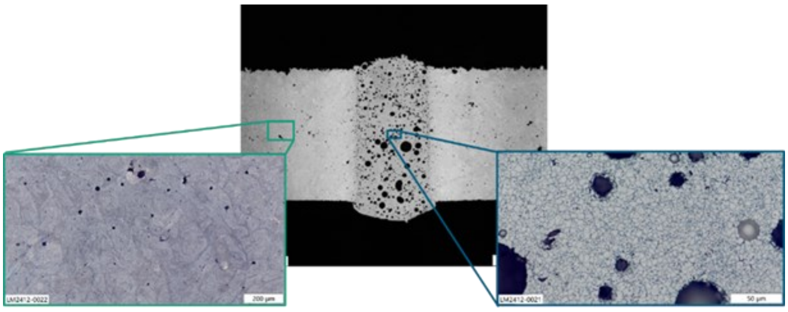

Fig. 4 Butt-Joint in AlZn5,5MgCu

A detailed investigation of the weld zone using SEM showed that the grains in the fusion zone had grown and that the grain boundaries had become covered. The base material, on the other hand, showed a fine grain structure (see Fig. 5).

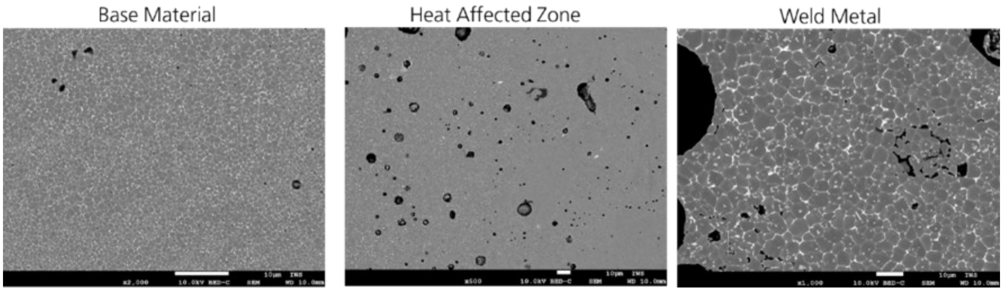

Fig. 5 : Left: base material; middle: HAZ: right: weld metal

3.2. Mechanical Properties

3.2.1. Tensile test

Laser beam welding was compared with three other welding processes as part of the study (Fig. 6). This comparison enables a comprehensive evaluation of the performance and efficiency of laser beam welding in relation to alternative techniques. The analysis focused on various parameters, including welding speed, weld quality, and the thermal effects on the material.
The tensile testing was conducted to determine the tensile strengths of welded specimens in the "as-welded" condition. The testing speed was set at 4 mm/min, with elongation measured using an extensometer. This method ensured accurate readings of the specimens' deformation under tensile loads.
The yield strength and tensile strength values can be found in Table 2. It can be seen that LBW and EBW as well as GTAW are at a very similar level, whereby the variance of the values for EBW stands out.
LBW and EBW samples also show mixed fractures in the HAZ and weld metal, whereas the samples from the GTAW process all fracture in the transition zone, as there is a large weld seam bulge (top surface and seam root).

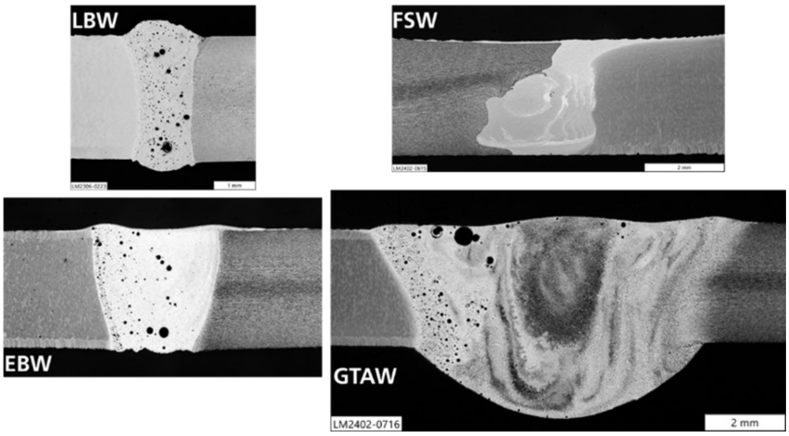

Fig. 6 Cross sections of butt-joints between AlSi7Mg0.6 and EN AW-5083 with different welding technologies (Laser beam welding –LBW, Friction stir welding – FSW, Electron beam welding – EBW, Gas tungsten arc welding – GTAW)

Table 2

	LBW	***FSW***	***EBW***	***GTAW***
Material combination	AlSi7Mg0.6 vs. EN AW-5083			
Power in kW	1,9	-	1,2	1,9
Welding speed in m/min	1,5	0,5	1,1	0,126
Yield strength in N/mm^2	155 ± 1	158 ± 0	157 ± 0	147 ± 2
Tensile strength in N/mm^2	214 ± 7	260 ± 10	210 ± 32	212 ± 11
Point of failure	HAZ / Weld Seam	Weld Seam	Weld Seam	HAZ

3.2.2. Fatigue tests

In addition to tensile testing, fatigue strength was assessed through fatigue testing of specimens in their "as-welded" condition. These tests were conducted using a resonance testing machine (Rumul Teststronic) operating at a frequency of approximately 88 Hz, with a load ratio of R = 0.1. To mitigate crack initiation at the lateral surfaces of the specimens, mechanical cold working was applied to the edges.

The following conclusions can be drawn from the results:

- A significant variability was observed in both laser beam welded (LBW) specimens, with failure locations and crack initiation occurring randomly within the weld seam, ranging from the seam center to the heat-affected zone (HAZ) and fusion line.
- When failure occurred in the vicinity of the fusion line, it typically originated within the additively manufactured (AM) material. In such instances, pores were identified on the fracture surface, indicating that the quality of the AM components has a direct impact on fatigue strength.
- Due to the pronounced variability observed, a Wöhler curve could not be established.

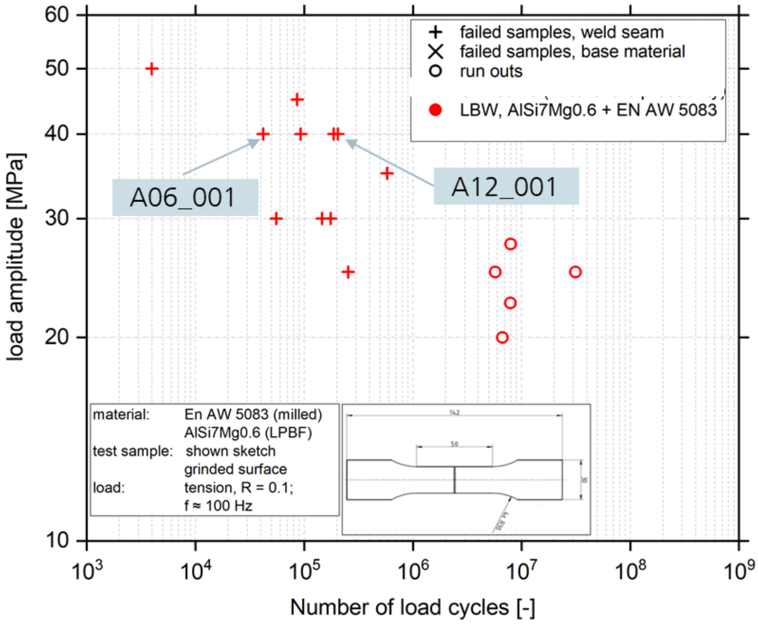

Fig. 7 Results of the fatigue strength tests on LBW specimens with fractured specimens at different load levels and run-outs

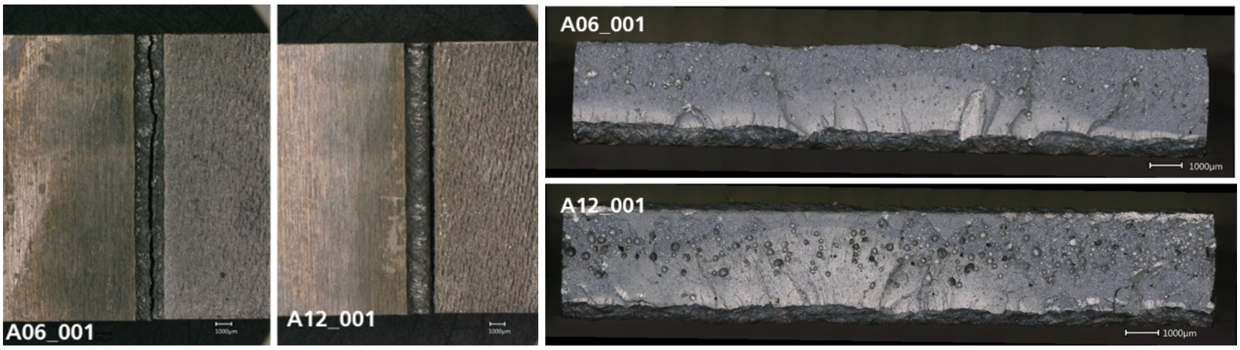

Fig. 8: Fracture types of the LBW samples

4. Demonstrator

The developed technology was tested on a demonstrator designed for a hydrogen application. The 3D-formed inlet facilitates the optimized flow of hydrogen into a test chamber, making it an ideal candidate for an additively manufactured (AM) application. Additionally, the standardized connector made of EN AW-5083 complies with industry standards, representing an effective solution for cost reduction within the assembly.
The demonstrator features both a radial and an axial weld, with the primary requirement for the weld joint being gas tightness. This means that there should be no open pre-canalizations or protrusions. The results of the welding trials are presented in Fig. 9, where it was possible to successfully transfer the experimental parameters previously determined on plate material. As a result, a Technology Readiness Level (TRL) of 6 has been achieved.

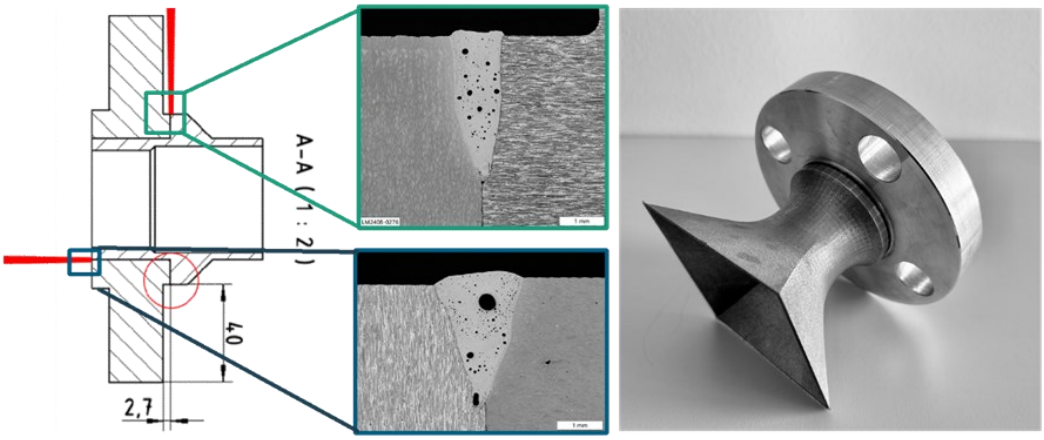

Fig. 9 Demonstrator with a radial and an axial weld between AlSi7Mg0,6 and EN AW-5083

5. Conclusion

In this study, the high quality of laser beam welding (LBW) for additively manufactured aluminum (AM) materials has been emphasized. It has been found that the quality of the base material, particularly its density and gas content, is crucial for the properties of the welded joint. By optimizing the material quality and adjusting the laser modulation parameters, the mechanical properties of the welds, such as porosity and strength, can be significantly improved.

The versatility of LBW applications in various sectors, including the energy sector and aerospace, underscores the potential of this technology. Compared to electron beam welding (EBW), LBW offers the advantage of not requiring a vacuum, and it outperforms gas tungsten arc welding (GTAW) in terms of heat input, leading to reduced distortion. Additionally, LBW enables welding of hot-crack-sensitive alloys without the need for filler material, which enhances process reliability.

In summary, the combination of advanced laser technology and the optimization of material properties presents a promising perspective for the production of high-quality welded joints across a variety of applications. Further research is needed to fully exploit the potential of this technology and to promote its application on an industrial scale.

Acknowledgements

The results presented were achieved in the project “WeldAlAM - Innovative Welding solutions for Aluminium Additive Manufactured light weight components” (CORNET: IGF- Vorhaben Nr.: 338 EBG / 1) (Walloon region SPW-Recherche (convention 2110232)).

Gefördert durch:
Bundesministerium für Wirtschaft und Klimaschutz
aufgrund eines Beschlusses des Deutschen Bundestages

References

[1] Kairet, T. & Godet, Stephane & Malet, Loic & Hemberg, A.. (2024). L-PBF Printing Of 7075 Aluminium Powder Modified Using A Pure Ti PVD Coating : In-Situ Micro-Alloying, In: Proceedings of EUROPM2024, EPMA, https://doi.org/10.59499/EP246274677

[2] Klumpp R. E., Akbarzadeh S., Kairet T., Ölmez V. , Gonon M., Mégret A., Delaunois F., Olivier M-G, Corrosion behavior of AlSi7Mg0.6 produced by selective laser melting: A comparative approach, Journal of Alloys and Compounds 1034 (2025) 181361

[3] Kairet T, Giaux R , Godet S , Malet L , Svarova P, Billy P, Keßler B, Dittrich D , Tiberto D , Hemberg A , L-PBF 3D PRINTING OF ALZN5,5MGCU (7075) ALUMINIUM MODIFIED WITH A TI-PVD COATING: IN-SITU MICROALLOYING, PRINTABILITY AND WELDABILITY ASSESSMENT OF THE ALLOY, ECSSMET2024, ESA Noordwijk,

[4] Boerner, S,; Dittrich, D.; Sahm, T.; Ullmann, L.; Kamm, P. H.; Jahn, A. (2025): X-Ray analysis of capillary and melt pool dynamics using laser beam iscillation welding for aluminium die-cast; In: Journal of Laser Applications. 37.